Theoretical spectroscopy and metastability of BeS and its cation

ARTICLE *in* CHEMICAL PHYSICS · AUGUST 2010

Impact Factor: 1.65 · DOI: 10.1016/j.chemphys.2010.05.006

5 AUTHORS, INCLUDING:

Hassen Ghalila
University of Tunis El Manar
21 PUBLICATIONS **53** CITATIONS
SEE PROFILE

Majdi Hochlaf
Université Paris-Est Marne-la-Vallée
240 PUBLICATIONS **1,592** CITATIONS
SEE PROFILE

Chemical Physics 373 (2010) 193–202

Contents lists available at ScienceDirect

Chemical Physics

journal homepage: www.elsevier.com/locate/chemphys

Theoretical spectroscopy and metastability of BeS and its cation

T. Larbi [a], F. Khadri [a], H. Ghalila [a], S. Lahmar [a,*], M. Hochlaf [b]

[a] Laboratoire de Spectroscopie Atomique, Moléculaire et Applications (LSAMA), Université Tunis El Manar, Faculté des Sciences de Tunis, Département de Physique, 1060, Tunisia
[b] Laboratoire Modélisation et Simulation Multi Echelle Université Paris-Est, MSME UMR 8208 CNRS, 5 bd Descartes, 77454 Marne-la-Vallée, France

ARTICLE INFO

Article history:
Received 28 January 2010
In final form 6 May 2010
Available online 12 May 2010

Dedicated to Prof. Zohra Ben Lakhdar for her retirement.

Keywords:
Ab initio calculations
Electronic structure
Spectroscopy
Diatomics

ABSTRACT

Multiconfiguration self-consistent field and multiconfiguration reference interaction including the Davidson's correction techniques were employed to calculate the potential energy curves (PECs) of the BeS/BeS^+ electronic states correlating to the 4/5 lowest dissociation limits. After nuclear motion treatment, we deduced reliable spectroscopic data for the neutral and cationic bound states. For BeS, the transition moments and spin-orbit couplings were also evaluated and used later with the PECs to deduce the rovibronic transition probabilities and the radiative lifetimes in the low-lying states, and to investigate the unimolecular decomposition processes of BeS ($X^1\Sigma^+$, $A^1\Pi$, $^3\Sigma^+$ and $B^1\Sigma^+$) leading to $Be(^1S_g) + S(^3P_g)$. The prominent mechanism is a spin-orbit induced predissociation via the repulsive $BeS(1^3\Sigma^-)$ state. Finally, we give the single ionization spectrum of BeS ($X^1\Sigma^+$) populating the BeS^+ ($X^2\Pi$, $1^2\Sigma^-$, $1^2\Sigma^+$, $1^2\Delta$, $2^2\Sigma^+$, $2^2\Pi$ and $3^2\Pi$) electronic states. The adiabatic ionisation energy of BeS is estimated to be ~9.15 eV.

1. Introduction

Beryllium Chalcogenides (such as BeS, BeSe and BeTe) were subject to several experimental and theoretical investigations because of their possible semi-conducting properties and their applications in microelectronic and optoelectronic devices such as the blue-green laser diodes. This is widely reviewed in Refs. [1–4] and references therein. Nevertheless, the diatomic gas phase building blocks of these 3D materials are less known.

In the present theoretical study, we treat the beryllium sulfide molecule, BeS, and its cation, BeS^+. In the literature, very few is available on their spectroscopy and metastability. Briefly, the $B^1\Sigma^+$ and $X^1\Sigma^+$ singlet electronic states of BeS molecule were identified in the absorption spectra of Gissane and Barrow [5]. Then, the lowest allowed triplet–triplet transition was observed and attributed by Cheetham et al. [6] to the $b^3\Pi - a^3\Pi$ transition. The $A^1\Pi$ state is also characterized [6]. Another electronic state of singlet spin multiplicity (namely the $C^1\Delta$) was located from perturbation of the $A^1\Pi$ state spectra. Theoretically, the results of the variational matrix Hartree–Fock calculations performed by Verhaegen and Richards [7] agree reasonably with previous observations. Later on, using hybrid experiment/deperturbation/*ab initio* calculations, Pouilly et al. [8], whose main purpose was to characterise the states responsible for the perturbations observed by Cheetham et al., have reassigned the observed triplet–triplet transition to the $^3\Delta$–$a^3\Pi$ rather than to the $b^3\Pi$–$a^3\Pi$ transition. In addition, they found that the main perturber of the $A^1\Pi$ state is not the lowest $^1\Delta$ state but the $a^3\Pi_2$ component. The electric properties of BeS ($X^1\Sigma^+$), including the dipole and quadrupole moments as well as the first and second polarisabilities, were calculated by Noga and Plutta [9]. So far, no studies are reported in the literature for the BeS^+ ion.

Presently, we perform state-of-the-art *ab initio* computations dealing with the potential energy curves (PECs) and wavefunctions of the lowest electronic states of BeS/BeS^+. Using highly correlated wavefunctions, we deduce their mutual spin–orbit couplings and dipole transition moments. For the bound states, rotational and vibrational parameters were evaluated after nuclear motion treatment, using both pertubative and variational approaches. Then, the PECs, the spin–orbit couplings and the dipole transition moments were used to deduce the radiative lifetimes for the vibrational levels of BeS ($a^3\Pi$, $A^1\Pi$, $^3\Sigma^+$ and $B^1\Sigma^+$) and the spin–orbit induced predissociation lifetimes for the $X^1\Sigma^+$, $A^1\Pi$ and $B^1\Sigma^+$ states crossed by the repulsive $1^3\Sigma^-$ state, correlating to the lowest dissociation asymptote. Finally, the single ionization spectrum of BeS was predicted. Very recently, similar works on the isovalent BeO/BeO^+ species were performed using similar methodologies [10,11], asserting the goodness of our predictions.

2. Computational details

The electronic calculations are done with the MOLPRO program suite [12]. We used the *spdfg*(*h*) cc-pV5Z basis sets for the description of the Be [13] and S [14] atoms. This results on 186 contracted

* Corresponding author. Tel.: +216 71746 551.
E-mail addresses: soulahmar@yahoo.fr (S. Lahmar), hochlaf@univ-mlv.fr (M. Hochlaf).

0301-0104/$ - see front matter © 2010 Published by Elsevier B.V.
doi:10.1016/j.chemphys.2010.05.006

Gaussian functions. We compute the electronic states using the state-averaged full valence complete active space self-consistent field (CASSCF) [15,16] followed by the internally contracted multi-reference configuration interaction (MRCI) approaches [17,18]. In the CASSCF approach, all electrons were correlated and the electronic states having the same spin multiplicity were averaged together with equal weights. At the MRCI level of theory, all configuration state functions (CSFs) from the CASSCF calculations were taken as reference and the Davidson correction (MRCI + Q) was considered for better accuracy [19]. The CASSCF wavefunctions have also been used to derive the dipole transition moments and the spin–orbit integrals in Cartesian coordinates, using the Breit-Pauli operator, as implemented in the MOLPRO program package.

The rovibrational spectra of the bound electronic states were deduced by solving the nuclear motion problem on our PECs and using either a standard perturbation approach and the derivatives of these PECs at equilibrium [20] or a variational treatment [21].

Later on, we incorporate our PECs, transition moments and spin–orbit couplings into the LEVEL and BCONT programs of LeRoy [22,23] to deduce the radiative lifetimes and the spin–orbit induced predissociation lifetimes of the lowest electronic states of BeS. Finally, the single ionization spectrum of BeS was deduced using our PEC of BeS ($X^1\Sigma^+$) and those of BeS^+ ($X^2\Pi$, $1^2\Sigma^+$, $1^2\Sigma^-$, $1^2\Delta$, $2^2\Sigma^+$, $2^2\Pi$ and $3^2\Pi$) with the LEVEL program.

3. Results

3.1. Potential energy curves of BeS and spectroscopy

Fig. 1 displays the MRCI + Q potential energy curves of the electronic states of BeS along the internuclear separation. These electronic states correlate to the $Be(^1S_g) + S(^3P_g)$, $Be(^1S_g) + S(^1D_g)$, $Be(^3P_u) + S(^3P_g)$ and $Be(^1S_g) + S(^1S_g)$ asymptotes. Presently, these asymptotes were positioned in energy using our calculations at the MRCI + Q level. These curves are given relative to the energy at the minimum of the ground state. Fig. 1 shows a high density of electronic states, especially for energies >3 eV. For more clarity, we plot in Fig. 2a–c the potentials of the singlets, the triplets and the quintets, respectively. Table 1 lists the dominant electron configurations of the 24 investigated electronic states. Among these states, seventeen (i.e. $X^1\Sigma^+$, $a^3\Pi$, $A^1\Pi$, $^3\Sigma^+$, $B^1\Sigma^+$, $1^3\Sigma^-$, $^3\Delta$, $C^1\Delta$, $1^1\Sigma^-$, $2^3\Sigma^-$, $b^3\Pi$, $2^1\Delta$, $2^1\Pi$, $1^5\Pi$, $2^1\Sigma^+$, $3^3\Pi$, $3^1\Pi$) are bound. They present potential wells for internuclear separation ranging from 3 to 7 bohr. Their equilibrium distances and excitation energies are also quoted in Table 1. The remaining states are found to be repulsive in nature.

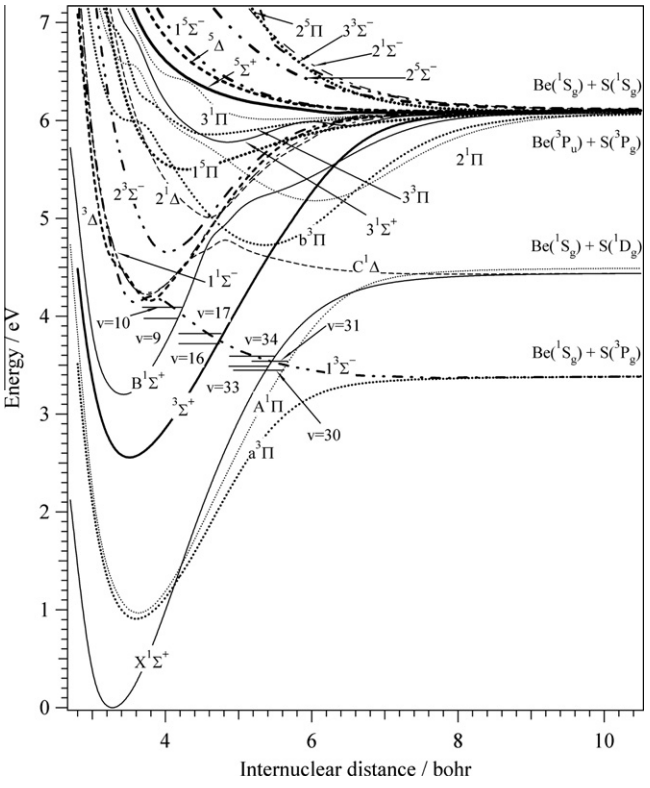

Fig. 1. MRCI + Q potential energy curves of the electronic states of BeS correlating to the four lowest dissociation limits. See text for details.

The electronic ground state of BeS is viewed to be the $X^1\Sigma^+$ followed by the close lying $a^3\Pi$ and $A^1\Pi$ states at ~1 eV. Our calculated excitation energies for these two excited states agree with previous experimental determinations [5,6,8]. Then, we locate a $^3\Sigma^+$ at 2.56 eV and the $B^1\Sigma^+$ at 3.20 eV. For internal energies of ~4 eV, we find a $^3\Delta$ state. This electronic state was not observed in the triplet–triplet absorption spectra of Cheetham et al. [6], which covered this energy domain, in despite that $^3\Delta$–$^3\Pi$ transitions are optically allowed. Our large calculations confirm the suggestion made by Pouilly et al. [8] of reassigning the observed bands to the $^3\Delta \rightarrow a^3\Pi$ transitions instead of the $b^3\Pi \rightarrow a^3\Pi$ ones. Indeed, our calculated $^3\Delta$–$a^3\Pi$ gap energy (i.e. 3.24 eV) coincides with the observed bands, with favorable Franck–Condon factors, whereas the $b^3\Pi$ is located distinctly higher in energy (~3.82 eV) and presents a potential well outside the Franck–Condon region of the $a^3\Pi$. When comparing BeS and its isovalent BeO [11] molecule, we have similar pattern of electronic states especially for the five lowest ones.

Because of the high density of the electronic states (cf. Fig. 1), vibronic and spin–orbit couplings are expected to take place between them. For the states, which belong to the same space symmetry and have the same spin multiplicity, these interactions result in mixings of their wavefunctions and avoided crossings between their potentials, leading to local minima, potential barriers ... For instance, the $C^1\Delta$ state presents a local minimum at 3.47 bohr (Fig. 2a)) and small potential barrier before reaching the $Be(^1S_g) + S(^1D_g)$ dissociation limit around 4.8 bohr. This barrier is due to an avoided crossing with the upper $2^1\Delta$. Moreover, the change in the behavior of the $b^3\Pi$ potential energy curve between 3.5 and 4 bohr is because of avoided crossings between the $b^3\Pi$ and the $3^3\Pi$, and higher $^3\Pi$ excited states, where vibronic couplings may take place. In addition, spin-orbit interactions such as the ones between the $X^1\Sigma^+$, $A^1\Pi$, $^3\Sigma^+$ and $B^1\Sigma^+$ and the repulsive $1^3\Sigma^-$ state may induce spin–orbit predissociations (see below).

From the derivatives at equilibrium of the bound states and standard second order perturbation theory, we deduced spectroscopic data including harmonic wavenumbers (ω_e), anharmonic terms ($\omega_e x_e$, $\omega_e y_e$), rotational constants (B_e, α_e) and dissociation energies (D_0). These data are listed in Table 2. Our calculated MRCI + Q equilibrium distances for the lowest electronic states deviate from the experimental values by less than 0.015 Å. Our harmonic wavenumbers for BeS ($X^1\Sigma^+$) and ($A^1\Pi$) states are calculated to be 1004.1 cm^{-1} and 773.9 cm^{-1}. These values are in accord with the estimated experimental wavenumbers of 997.4 cm^{-1} and 762.5 cm^{-1} of Refs. [5,6,8]. However, a relatively large difference between our calculated and measured ω_e values is found for the B state. Close examination of the potential energy curve of this state shows that it presents a strong anharmonic behavior and is hence far from a standard morse type potential. This is due to the interaction of this electronic state with the other $^1\Sigma^+$ singlet states, as mentioned in Ref. [8]. Indeed, the *B* state is dominantly described by the $(4\sigma)^2(5\sigma)^2(6\sigma)^1(7\sigma)^1(2\pi)^4$ electron configuration

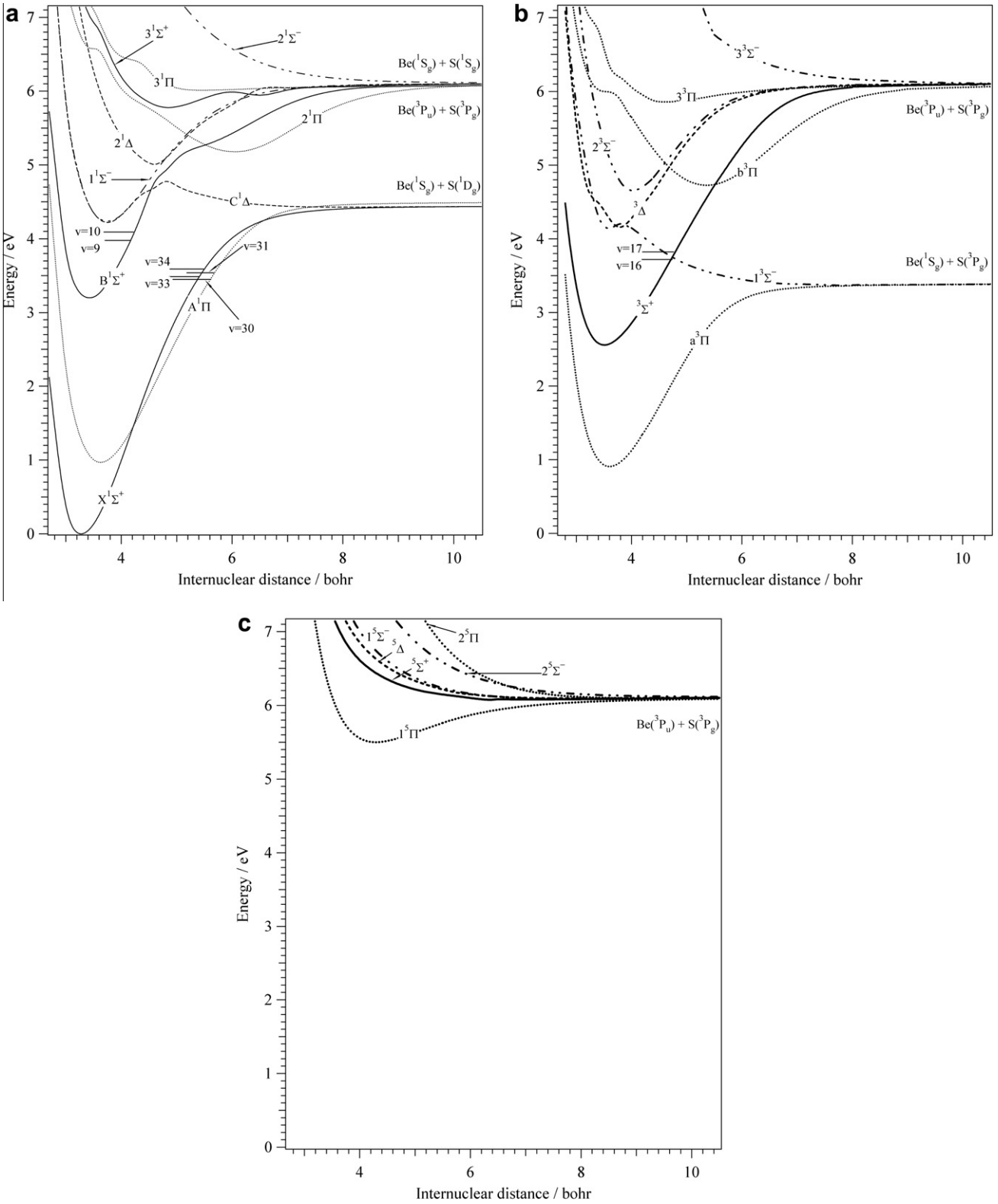

Fig. 2. MRCI + Q potential energy curves of the electronic states of BeS of singlet (a), triplet (b) and quintet (c) spin multiplicities. See text for details.

for short internuclear distances. The weight of this configuration is decreasing in favor of another configuration by lengthening the BeS distance: The CI coefficient corresponding to this configuration in the CASSCF wavefunction varies from 0.61 to 0.58 to 0.53 for R = 3.2, 3.6 and 4.0, respectively. Table 2 shows also that our $\omega_e x_e$ values are not in agreement with experiment. In addition to the distortion of our calculated adiabatic potential energy curves due to the muticonfigurational character of the wave functions, the disagreement between experimental and theoretical spectroscopic constants in general, and $\omega_e x_e$ values in particular, might be attributed to the fitting procedures and which experimental frequencies are considered.

Table 1
Dominant electron configuration of the investigated electronic states of BeS. The equilibrium distances, r_e, are in Å and the MRCI + Q excitation energies (T in eV) are also given for the bound states.

State	Electron configuration[a]	r_e	T[b]
$X^1\Sigma^+$	$(4\sigma)^2(5\sigma)^2(6\sigma)^2(2\pi)^4$	1.73	0.000
		1.745[cd]	
		1.7415[e]	
$a^3\Pi$	$(4\sigma)^2(5\sigma)^2(6\sigma)^2(2\pi)^3(7\sigma)^1$	1.92	0.907
		1.9190[f]	0.880[f]
			0.329[g]
$A^1\Pi$	$(4\sigma)^2(5\sigma)^2(6\sigma)^2(2\pi)^3(7\sigma)^1$	1.92	0.966
		1.907[e]	0.987[e]
		1.9087[f]	0.488[g]
$^3\Sigma^+$	$(4\sigma)^2(5\sigma)^2(6\sigma)^1(2\pi)^4(7\sigma)^1$	1.88	2.556
			2.032[g]
$B^1\Sigma^+$	$(4\sigma)^2(5\sigma)^2(6\sigma)^1(2\pi)^4(7\sigma)^1$	1.81	3.201
		1.818[cd]	3.207[hd]
		1.8136[i]	3.216[e]
			2.931[g]
$1^3\Sigma^-$	$(4\sigma)^2(5\sigma)^2(6\sigma)^2(2\pi)^3(3\pi)^1$	1.90	4.14
$^3\Delta$	$(4\sigma)^2(5\sigma)^2(6\sigma)^2(2\pi)^3(3\pi)^1$	1.94	4.158
			4.098[f]
			3.966[g]
$C\ ^1\Delta$	$(4\sigma)^2(5\sigma)^2(6\sigma)^2(2\pi)^3(3\pi)^1$	1.99	4.220
		2.005[i]	1.679[i]
$1^1\Sigma^-$	$(4\sigma)^2(5\sigma)^2(6\sigma)^2(2\pi)^3(3\pi)^1$	1.98	4.239
$2^3\Sigma^-$	$(4\sigma)^2(5\sigma)^2(6\sigma)^2(2\pi)^2(7\sigma)^2$	2.13	4.655
$b^3\Pi$	$(4\sigma)^2(5\sigma)^2(6\sigma)^1(2\pi)^4(3\pi)^1$	2.83	4.726
$2^1\Delta$	$(4\sigma)^2(5\sigma)^2(6\sigma)^2(2\pi)^2(7\sigma)^2$	2.47	5.008
$2^1\Pi$	$(4\sigma)^2(5\sigma)^2(6\sigma)^2(2\pi)^3(8\sigma)^1$	3.20	5.178
$1^5\Pi$	$(4\sigma)^2(5\sigma)^2(6\sigma)^2(2\pi)^2(7\sigma)^1(3\pi)^1$	2.27	5.500
$3^1\Sigma$	$(4\sigma)^2(5\sigma)^2(6\sigma)^2(2\pi)^2(7\sigma)^2$	2.57	5.770
$3^3\Pi$	$(4\sigma)^2(5\sigma)^2(6\sigma)^2(2\pi)^3(8\sigma)^1$	2.44	5.856
$3^1\Pi$	$(4\sigma)^2(5\sigma)^2(6\sigma)^1(2\pi)^4(3\pi)^1$	2.90	6.012
$^5\Sigma^+$	$(4\sigma)^2(5\sigma)^2(6\sigma)^1(2\pi)^3(7\sigma)^1(3\pi)^1$	–	–
$^5\Delta$	$(4\sigma)^2(5\sigma)^2(6\sigma)^1(2\pi)^3(7\sigma)^1(3\pi)^1$	–	–
$1^5\Sigma^-$	$(4\sigma)^2(5\sigma)^2(6\sigma)^1(2\pi)^3(7\sigma)^1(3\pi)^1$	–	–
$2^5\Sigma^-$	$(4\sigma)^2(5\sigma)^2(6\sigma)^2(2\pi)^2(7\sigma)^1(8\sigma)^1$	–	–
$2^5\Pi$	$(4\sigma)^2(5\sigma)^2(6\sigma)^1(2\pi)^3(7\sigma)^1(8\sigma)^1$	–	–
$3^3\Sigma^-$	$(4\sigma)^2(5\sigma)^2(6\sigma)^1(2\pi)^3(7\sigma)^1(3\pi)^1$	–	–
$2^1\Sigma^-$	$(4\sigma)^2(5\sigma)^2(6\sigma)^2(2\pi)^2(7\sigma)^1(8\sigma)^1$	–	–

[a] Dominant electron configuration quoted at the equilibrium distance of the ground state.
[b] Calculated as the difference between the energy of the minimum of the ground state and the minimum of the considered electronic state.
[c] Experimental r_0 value.
[d] Exp. [5].
[e] Exp. [6].
[f] Deduced by Pouilly et al. [8] from experimental results of Cheetham et al. [6].
[g] Theo. [8].
[h] Experimental T_0 value.
[i] Exp. [26].

Table 2
MRCI + Q spectroscopic constants of the bound electronic state of BeS including the harmonic wavenumber (ω_e), the anharmonic terms ($\omega_e x_e$, $\omega_e y_e$), the rotational constants (B_e, α_e), the dissociation energies (D_0). All values are in cm^{-1} except if specified.

States	ω_e	$\omega_e x_e$	$\omega_e y_e$	B_e	α_e	D_0 (eV)
$X^1\Sigma^+$	1004.1	17.78	1.87	0.798	0.014	4.37
[a]	997.94	6.137	–	0.79059	0.00664	–
[b]	997.4	6.3	–	0.787[c]	–	–
[d]	891	7.7		0.749		
$a^3\Pi$	797.4	38.73	4.54	0.654	0.003	2.41
[d]	723	8.7		0.637		
[e]	737	4.1		0.6511	0.0058	
$A^1\Pi$	773.9	16.33	1.63	0.649	0.003	3.46
[a]	762.46	4.12	–	0.659	0.00605	–
[d]	747	7.5		0.639		
[e]	762.13	4.09		0.6581	0.00583	
$^3\Sigma^+$	687.7	12.64	2.34	0.676	0.017	3.49
[d]	760	13.3		0.680		
$B^1\Sigma^+$	691.4	51.29	7.12	0.732	0.005	2.83
[a]	851.35	4.85	–	0.72894	0.00604	–
[b]	850.4	4.9	–	0.7258[c]	–	–
[d]	900	8.2		0.742		
$^3\Delta$	705.6	4.43	0.80	0.635	0.009	1.87
$C^1\Delta$	636.1	8.17	2.25	0.606	0007	0.19
[a]	660.7	5.5	–	0.5963	0.0069	–
$1^1\Sigma^-$	649.3	6.37	1.54	0.610	0.005	1.81
$2^3\Sigma^-$	778.4	5.06	1.62	0.528	0.0005	1.39
$b^3\Pi$	398.1	7.99	0.62	0.299	0.001	1.35
$2^1\Delta$	596.1	5.22	0.24	0.393	0.006	1.03
$2^1\Pi$	306.3	1.84	0.05	0.234	0.001	0.87
$1^5\Pi$	364.7	7.13	0.03	0.466	0.011	0.57
$3^1\Sigma^+$	390.6	8.30	0.61	0.364	0.001	0.29
$3^3\Pi$	267.9	8.42	0.06	0.403	0.024	0.22
$3^1\Pi$	127.2	9.01	0.33	0.285	0.023	0.08

[a] Exp. [26].
[b] Exp. [5].
[c] Experimental B_0 value.
[d] [8].
[e] Deduced by Pouilly et al. [8] from experimental results of Cheetham et al. [6].

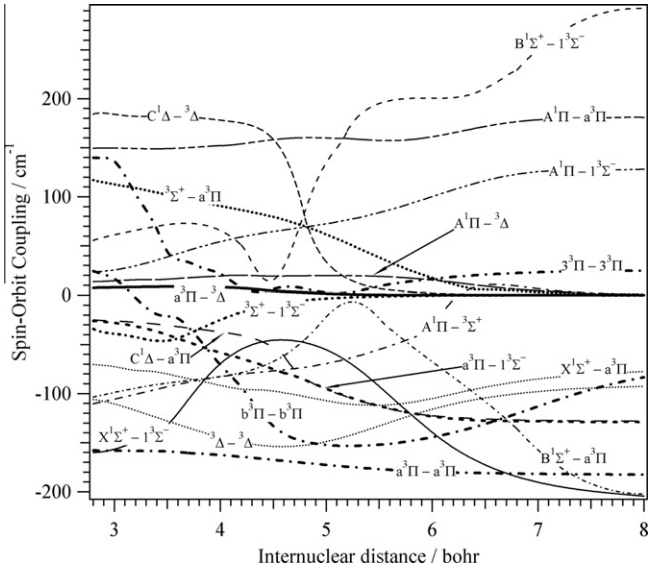

Fig. 3. Evolution of the non-vanishing spin–orbit integrals between the lowest electronic states of BeS versus the internuclear distance.

3.2. BeS spin–orbit couplings

Since the spin-orbit constant of the sulphur atom in the ^3P_g ground state equals 382.4 cm^{-1} [24], the S atom may induce significant relativistic effects in the spectroscopy of sulphur bearing molecules. Presently, the non-vanishing spin–orbit integrals, evaluated over the CASSCF wavefunctions and involving the lowest electronic states of BeS were calculated. They are presented in Fig. 3. We use the following notation: i–j denotes the $\langle i|\mathbf{H^{SO}}|j\rangle$ integral. For instance, the $C^1\Delta$–$a^3\Pi$ term corresponds to the $\langle C^1\Delta|\mathbf{H^{SO}}|a^3\Pi\rangle$ integral. For the lowest crossing states we give in Table 3 the BeS crossing internuclear distance R_c, the spin–orbit integral at R_c and at $R_c \pm 0.4$ bohr, and the dominant electronic configuration at R_c for the i and j crossing states.

As already demonstrated in Ref. [8], Fig. 3 and Table 3 show that the spin–orbit couplings are not negligible. Several of these integrals amount to more than 50 cm^{-1}. Therefore, spin–orbit conversions between the BeS electronic states may occur. We expect that

Table 3
Spin orbit integrals $|\langle i|\mathbf{H^{SO}}|j\rangle|$ calculated (in cm^{-1}) for the lowest crossing states of BeS, at the crossing internuclear distance R_c (in bohr), R_c – 0.4 bohr and R_c + 0.4 bohr. The dominant electronic configuration of the *i* and *j* crossing states are also given at R_c.

Crossing states		R_c (bohr)	$\|\langle i\|\mathbf{H^{SO}}\|j\rangle\|$ (cm^{-1}) at:			Dominant electronic configuration at R_c	
i	*j*		$R_c - 0.4$	R_c	$R_c + 0.4$	State *i*	State *j*
$X^1\Sigma^+$	$a^3\Pi$	4.12	85	94	98	$(6\sigma)^2(2\pi)^4$	$(6\sigma)^2(2\pi)^3(7\sigma)^1$
$1^3\Sigma^-$	$A^1\Pi$	5.65	77	88	102	$(6\sigma)^2(2\pi)^2(7\sigma)^2$	$(6\sigma)^2(2\pi)^3(7\sigma)^1$
$X^1\Sigma^+$	$1^3\Sigma^-$	5.45	58	88	126	$(6\sigma)^2(2\pi)^4$	$(6\sigma)^2(2\pi)^2(7\sigma)^2$
$1^3\Sigma^-$	$^3\Sigma^+$	4.74	13	6	3	$(6\sigma)^2(2\pi)^2(7\sigma)^2$	$(6\sigma)^1(2\pi)^4(7\sigma)^1$
$B^1\Sigma^+$	$1^3\Sigma^-$	4.20	72	51	29	$(6\sigma)^1(2\pi)^4(7\sigma)^1$	$(6\sigma)^2(2\pi)^2(7\sigma)^2$

such couplings play a role in the perturbations of the BeS electronic states, for instance via predissociation processes (see Section 4.1.2 for more details.). For some of off-diagonal terms, our integrals are off by 50% when compared to those of Ref. [8]. This is not surprising: For the upper states, they present more or less a diffuse nature (valence – Rydberg character) that is accounted for sufficiently enough with our large basis set and not previously. For the SH molecule, we showed recently that the inclusion of these diffuse basis functions is mandatory for the accurate computation of these spin–orbit couplings [25]. We refer to Ref. [25] for a wide discussion.

Finally, we calculate the spin–orbit constant at equilibrium ($A_{SO,e}$) for the $^3\Pi$ electronic states of BeS. This constant is deduced from the corresponding diagonal spin–orbit integral evaluated at equilibrium and using the formula of Ref. [24]. Our values are: $A_{SO,e}$ ($a^3\Pi$) = −160, $A_{SO,e}$ ($b^3\Pi$) = −147 and $|A_{SO,e}|$ ($3^3\Pi$) = 6 (all values are in cm^{-1}). For the $a^3\Pi$, our spin–orbit constant is in agreement with the -180 ± 20 cm^{-1} experimental value [8].

3.3. Potential energy curves of BeS^+ and spectroscopy

Fig. 4 depicts the MRCI + Q PECs of the electronic states of BeS^+ correlating to the five lowest dissociation limits ($Be^+(^2S_g) + S(^3P_g)$, $Be(^1S_g) + S^+(^4S_u)$, $Be^+(^2S_g) + S(^1D_g)$, $Be^+(^2S_g) + S(^1S_g)$ and $Be(^1S_g) + S^+(^2D_u)$). These asymptotes are located using our calculations on the separated atoms. For more clarity, we have plotted separately on Fig. 5a and b the curves corresponding to the doublets and the quartets, respectively. Table 4 presents the dominant electron configuration of these electronic states, quoted at the equilibrium distance of BeS^+ ground state, and their excitation energies. Our calculations show that the BeS^+ ground state is the $X^2\Pi$ corresponding to the removal of an electron from the outermost 2π molecular orbital (MO) of BeS. The first excited state is the $1^4\Sigma^-$ corresponding to the ejection of an electron from the 2π MO and simultaneous excitation of a second one into the vacant 7σ. The quartet is followed by the $1^2\Sigma^-$ and the $1^2\Sigma^+$ states. Inspection of Fig. 4 reveals that the $X^2\Pi$, $1^4\Sigma^-$, $1^2\Sigma^-$ and $1^4\Pi$ states, which correlate adiabatically to the lowest dissociation limit $\{Be^+(^2S_g) + S(^3P_g)\}$ are bound. For the isovalent BeO^+ cation [10], the $1^4\Pi$ state is repulsive in nature. This difference may be explained after examination of the corresponding wavefunctions in the molecular region. For instance, our calculations [10] show that the $BeO^+(1^4\Pi)$ is dominantly described by the $(3\sigma)^2(4\sigma)^1(5\sigma)^1(1\pi)^3$ electron configuration. However, the $BeS^+(1^4\Pi)$ state wavefunction is dominated by two configurations: $(5\sigma)^2(6\sigma)^1(7\sigma)^1(2\pi)^3$ and the $(5\sigma)^2(6\sigma)^2(2\pi)^2(3\pi)^1$ (CI coefficients: 0.96 and 0.2 in the CASSCF calculations) where the 6σ and the 7σ molecular orbitals are strongly localized on the sulphur and the beryllium atoms, respectively. The $(5\sigma)^2(6\sigma)^2(2\pi)^2(3\pi)^1$ configuration corresponds, hence, to a charge transfer from the Be atom towards the S atom, due to interaction with a higher ionic $^4\Pi$ state going down from the $S^- + Be^{++}$ asymptote (not shown here) to the molecular region.

For energies >2 eV, we predict the existence of several other cationic bound states (see Fig. 4). Moreover, this figure shows that the ground state is well isolated from all other states, whereas the electronically excited BeS^+ states are gathered into groups. Several interactions are expected between them by vibronic and spin–orbit couplings.

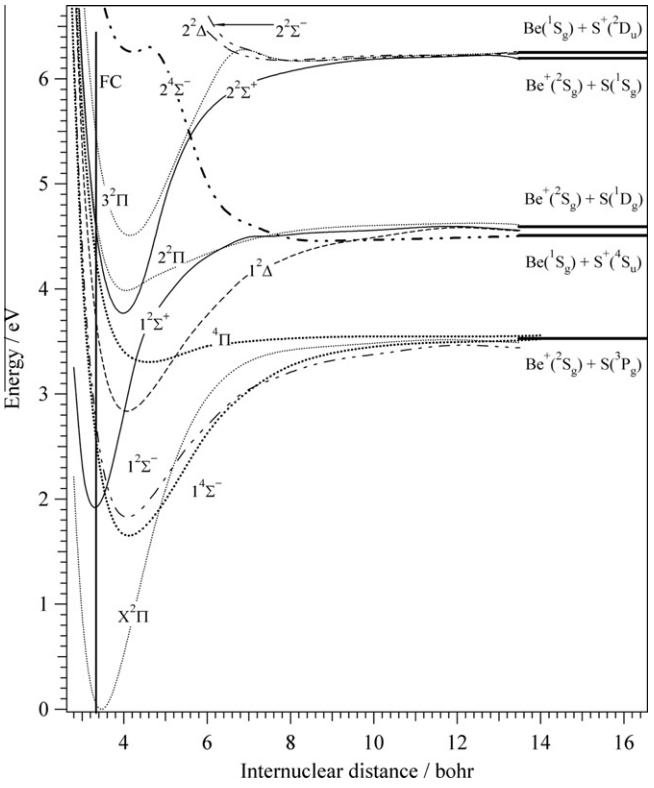

Fig. 4. MRCI + Q potential energy curves of the electronic states of BeS^+ correlating to the five lowest dissociation limits. The vertical solid line corresponds to the middle of the Franck–Condon (FC) zone, i.e. the maximum of the BeS ($X\ ^1\Sigma^+$, $v = 0$) wavefunction.

We give in Table 4 the equilibrium distances of the bound states of BeS^+. For $BeS^+(X^2\Pi)$, we compute R_e = 1.83 Å, which is slightly longer than its value in the neutral ground state. For the $X^2\Pi$, $1^4\Sigma^-$, $1^2\Sigma^-$, $1^2\Sigma^+$, $1^2\Delta$, $1^4\Pi$, $2^2\Sigma^+$, $2^2\Pi$ and $3^2\Pi$ electronic states, we deduced a set of spectroscopic constants (Table 5). Our data are predictive in nature and should have similar accuracy as discussed above for the neutral molecule.

Finally, Fig. 6 presents the evolution of the non-vanishing spin-orbit integrals involving the lowest electronic states of BeS^+. Numerical values of these integrals are given in Table 6 for the lowest crossing electronic states at the crossing BeS internuclear distance R_c and $R_c \pm 0.4$ bohr. These data might be useful to understand some of the mutual interactions between these electronic states as pointed out above. Especially, they allow the evaluation of the spin–orbit constants at equilibrium for the doubly degenerate states. For $BeS^+(X^2\Pi)$, we compute a spin–orbit con-

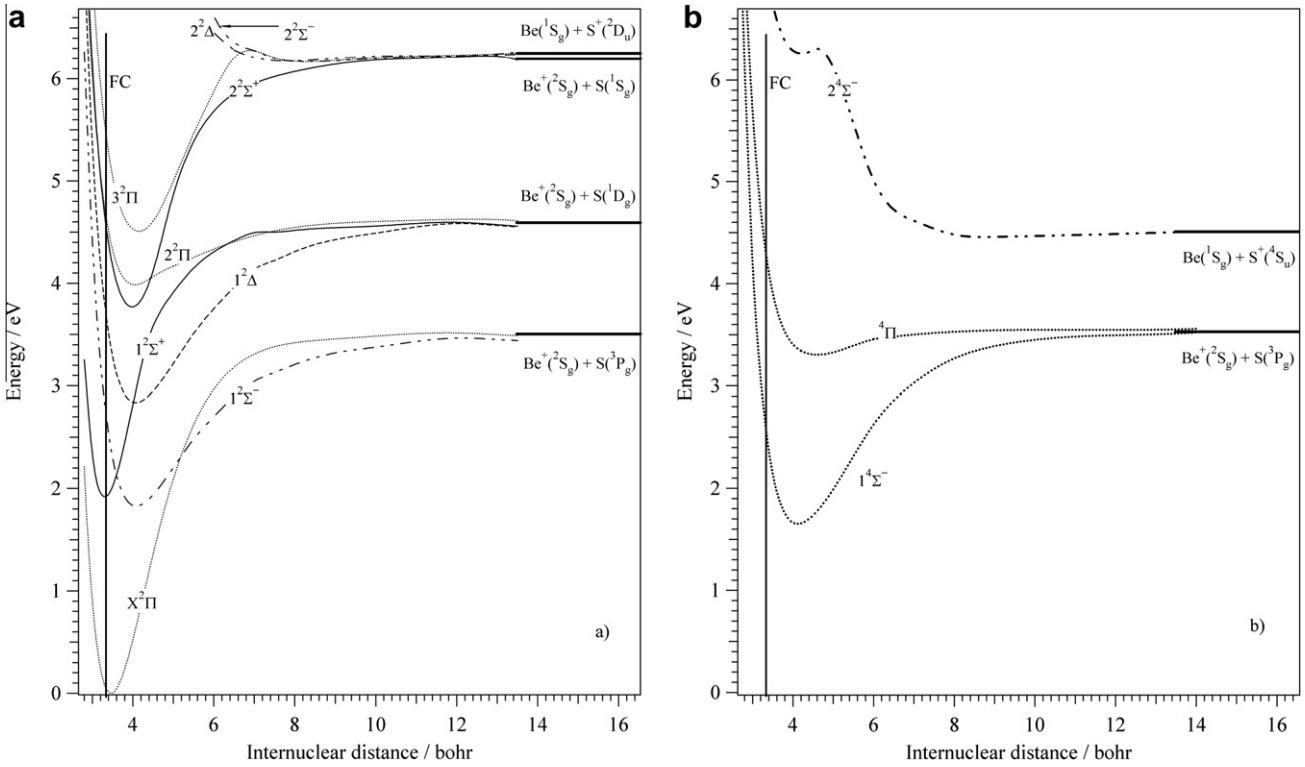

Fig. 5. MRCI + Q potential energy curves of the electronic states of BeS^+ of doublet (a) and quartet (b) spin multiplicities.

Table 4
Dominant electron configuration of the investigated electronic states of BeS^+. The equilibrium distances, r_e are in Å and the MRCI + Q excitation energies (T in eV) are also given for the bound states.

State	Electron configuration[a]	r_e	T[b]
$X^2\Pi$	$(4\sigma)^2(5\sigma)^2(6\sigma)^2(2\pi)^3$	1.83	0.0
$1^4\Sigma^-$	$(4\sigma)^2(5\sigma)^2(6\sigma)^2(2\pi)^2(7\sigma)^1$	2.18	1.651
$1^2\Sigma^-$	$(4\sigma)^2(5\sigma)^2(6\sigma)^2(2\pi)^2(7\sigma)^1$	2.16	1.829
$1^2\Sigma^+$	$(4\sigma)^2(5\sigma)^2(6\sigma)^1(2\pi)^4$	1.75	1.921
$1\ ^2\Delta$	$(4\sigma)^2(5\sigma)^2(6\sigma)^2(2\pi)^2(7\sigma)^1$	2.16	2.836
$1^4\Pi$	$(4\sigma)^2(5\sigma)^2(6\sigma)^1(2\pi)^3(7\sigma)^1$	2.44	3.303
$2^2\Sigma^+$	$(4\sigma)^2(5\sigma)^2(6\sigma)^2(2\pi)^2(7\sigma)^1$	2.11	3.769
$2^2\Pi$	$(4\sigma)^2(5\sigma)^2(6\sigma)^1(2\pi)^3(7\sigma)^1$	2.14	3.985
$3^2\Pi$	$(4\sigma)^2(5\sigma)^2(6\sigma)^1(2\pi)^3(7\sigma)^1$	2.20	4.508
$2^4\Sigma^-$	$(4\sigma)^2(5\sigma)^2(6\sigma)^1(2\pi)^3(3\pi)^1$	–	–
$2\ ^2\Delta$	$(4\sigma)^2(5\sigma)^2(6\sigma)^1(2\pi)^3(3\pi)^1$	–	–
$2^2\Sigma^-$	$(4\sigma)^2(5\sigma)^2(6\sigma)^1(2\pi)^3(3\pi)^1$	–	–

[a] Dominant electron configuration quoted at the equilibrium distance of the ground state.
[b] Calculated as the difference between the energy of the minimum of the ground state and the minimum of the considered electronic state.

Table 5
MRCI + Q spectroscopic constants of the electronic states of BeS^+ including the harmonic wavenumber (ω_e), the anharmonic terms ($\omega_e x_e$, $\omega_e y_e$), the rotational constants (B_e, α_e), the dissociation energies (D_0) and spin–orbit constant at equilibrium geometry ($|A_{SO}|$). All values are in cm^{-1} except if specified.

States	ω_e	$\omega_e x_e$	$\omega_e y_e$	B_e	α_e	D_0 (eV)	$\lvert A_{SO}\rvert$
$X^2\Pi$	865.60	1.19	0.46	0.713	0.006	3.46	310
$1^4\Sigma^-$	464.45	7.05	0.63	0.505	0.008	1.83	–
$1^2\Sigma^-$	486.91	4.85	0.03	0.513	0.007	1.60	–
$1^2\Sigma^+$	980.27	11.35	0.29	0.784	0.011	2.61	–
$1^2\Delta$	484.85	4.78	0.009	0.515	0.007	1.71	2
$1^4\Pi$	237.81	5.47	0.19	0.404	0.004	0.23	121
$2^2\Sigma^+$	604.31	4.09	0.23	0.538	0.0001	2.42	–
$2^2\Pi$	438.04	19.28	0.20	0.523	0.012	0.61	36
$3^2\Pi$	494.76	2.75	0.31	0.497	0.001	1.71	38

stant at equilibrium $|A_{SO,e}| = 310\ cm^{-1}$. The last column of Table 5, lists the $|A_{SO,e}|$ values for the $1^2\Delta$, $1^4\Pi$, $2^2\Pi$ and $3^2\Pi$ states.

4. Discussion

In the literature, perturbations in the ro-vibrational levels of BeS are noticed due to the mutual interaction of the electronic excited states. The knowledge of accurate transition probabilities and rovibrational level lifetimes are of great interest for the quantitative interpretation of these perturbations. In the following, we will focus on the determination of the radiative lifetimes of the $A^1\Pi$, $B^1\Sigma^+$, $a^3\Pi$ and $^3\Sigma^+$ states and, then, the spin–orbit induced predissociation lifetimes of the $X^1\Sigma^+$, $A^1\Pi$, and $B^1\Sigma^+$ states. Finally, we give the single ionization spectrum of BeS.

4.1. Natural lifetimes of the $A^1\Pi$, $B^1\Sigma^+$, $a^3\Pi$ and $^3\Sigma^+$ states of BeS

4.1.1. Radiative lifetimes

Fig. 7 shows the evolution, versus the internuclear distance, of our calculated dipole transition moments between the $X^1\Sigma^+$, $A^1\Pi$ and $B^1\Sigma^+$ states. The optically allowed emission transitions are $A \rightarrow X$, $B \rightarrow X$ and $B \rightarrow A$. These data are incorporated together with our potential energy curves into the LeRoy's LEVEL program, in order to deduce the radiative emission probabilities between each couple of vibronic v' and v'' levels. The radiative lifetime $\tau^{rad,v'}$ of a v' vibrational level is then deduced by:

$$\tau^{rad,v'} = \sum_{v''} \frac{1}{A_{v'v''}}$$

where $A_{v'v''}$ corresponds to the Einstein coefficient of spontaneous emission from the v' to the v'' levels.

Our calculated radiative lifetimes for the $A^1\Pi$ and $B^1\Sigma^+$ vibrational levels are reported in Tables 7 and 8, respectively, as well as their variationally calculated energies. The vibrational levels of

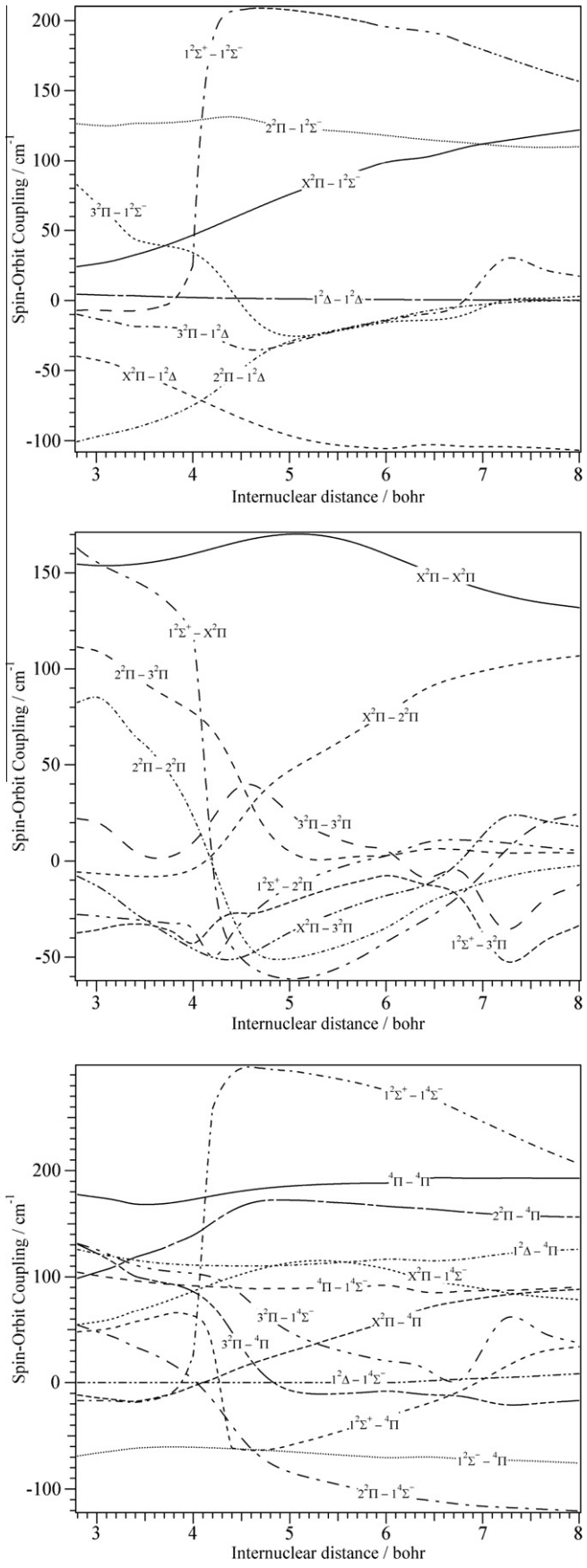

Fig. 6. Evolution of the non-vanishing spin–orbit integrals between the investigated states of BeS^+ versus the internuclear distance.

the $B^1\Sigma^+$ state can decay via radiative transitions populating either the A or the X states. For this electronic state, the radiative lifetimes $\tau^{\mathrm{rad},v'}$ are expressed as:

$$\frac{1}{\tau^{\mathrm{rad},v'}} = \frac{1}{\tau^{\mathrm{rad},v'}_{B\to A}} + \frac{1}{\tau^{\mathrm{rad},v'}_{B\to X}}$$

Table 7 shows that the radiative lifetimes of the $A^1\Pi$ vibrational levels are decreasing smoothly from 240 ns till 100 ns for $0 \leqslant v' \leqslant 33$. For the ro-vibrational levels of the $B^1\Sigma^+$, we compute radiative lifetimes of few ns.

A forbidden $i \to X$ transition, such as $a^3\Pi \to X^1\Sigma^+$ and $^3\Sigma^+ \to X^1\Sigma^+$, can borrow its ability to radiate from remote j states via allowed $j \to X$ transitions and spin–orbit coupling $\langle j|H^{SO}|i\rangle$ between the i and j states. The lifetime τ_i of the i state can be estimated by the formula [24]:

$$\tau_i = \left(\frac{E_j - E_i}{\langle j|\mathbf{H}^{SO}|i\rangle}\right)^2 \frac{v^3(i-X)}{v^3(j-X)}\tau_j$$

where E_j–E_i is the energy difference between the i and j electronic states. For the $a^3\Pi$ state, it may borrow its radiative rate from both the A and B singlet states. Our estimated lifetime for the $a^3\Pi$ state is of few microseconds. For the $^3\Sigma^+$, longer radiative lifetimes are predicted since the spin–orbit coupling with the upper $B^1\Sigma^+$ is vanishing.

4.1.2. Spin–orbit induced predissociation of the $X^1\Sigma^+$, $A^1\Pi$, and $B^1\Sigma^+$ states by the $1^3\Sigma^-$

Fig. 1 shows that the $X^1\Sigma^+$ and the $A^1\Pi$ states correlate adiabatically to the second dissociation limit and, that the $^3\Sigma^+$ and $B^1\Sigma^+$ states converge to the third one, where as the $a^3\Pi$ and $1^3\Sigma^-$ states correlate to the ground asymptote $\{Be(^1S_g) + S(^3P_g)\}$. The $X^1\Sigma^+$, $A^1\Pi$, $^3\Sigma^+$ and $B^1\Sigma^+$ electronic states are crossed by the repulsive $1^3\Sigma^-$ state, which leads directly to the lowest dissociation limit. At these crossings, spin–orbit induced predissociation processes via this repulsive state may take place. Fig. 3 shows that the spin–orbit integrals involving these bound states and this repulsive state are significant, particularly in the region immediately close to their respective crossings (i.e. BeS distances 5.44, 5.6, 4.7 and 4.2 bohr, respectively, Fig. 1). The PECs of these states together with their spin–orbit couplings are incorporated into the LeRoy's BCONT program. We deduce hence the non-radiative predissociative lifetimes $\tau^{\mathrm{non\text{-}rad},v'}$ of these vibrational levels. The lifetimes $\tau^{v'}$ are calculated using

$$\frac{1}{\tau^{v'}} = \frac{1}{\tau^{\mathrm{rad},v'}} + \frac{1}{\tau^{\mathrm{non\text{-}rad},v'}}$$

For the $X^1\Sigma^+$ ground state, this crossing occurs for relatively high vibrational levels, i.e. those located above the $Be(^1S_g) + S(^3P_g)$ limit. Our calculations reveal that the lowest predissociated vibrational level is the $v' = 34$. The natural lifetimes of this level equals 420 μs. For the $v' = 35$ and 36 upper levels, their lifetimes decrease rapidly to 83 and 17 ns due to spin–orbit induced predissociation by the $1^3\Sigma^-$.

For the $A^1\Pi$ and $B^1\Sigma^+$ states, our computed predissociative lifetimes are listed in Tables 7 and 8, respectively, as well as their corresponding natural lifetimes $\tau^{\mathrm{nat},v'}$. Tables 7 and 8 and Fig. 1 show that the crossings between the A and the $1^3\Sigma^-$ states and between the B and $1^3\Sigma^-$ states occur in the vicinity of $30 < v' < 31$ and $9 < v' < 10$, respectively. For these levels we gave in previous section their $\tau^{\mathrm{nat},v'}$, which are mainly due to radiative desexcitations. However, for the $A^1\Pi$ ($v' = 30$) and the $B^1\Sigma^+$ ($v' = 9$) there is a competition between the radiative and spin–orbit processes, leading to lifetimes in the same order of magnitude (ns timescale). For the upper vibrational levels located immediately above the crossings,

Table 6
Spin orbit integrals $|\langle i|\mathbf{H}^{SO}|j\rangle|$ calculated (in cm^{-1}) for the lowest crossing states of BeS^+, at the crossing internuclear distance R_c (bohr), R_c – 0.4 bohr and R_c + 0.4 bohr. The dominant electronic configuration of the *i* and *j* crossing states are also given at R_c.

Crossing states		R_c (bohr)	$\|\langle i\|\mathbf{H}^{SO}\|j\rangle\|(cm^{-1})$ at:			Dominant electronic configuration at R_c	
State *i*	State *j*		R_c–0.4	R_c	R_c + 0.4	State *i*	State *j*
$X^2\Pi$	$1^4\Sigma^-$	4.86	101	111	115	$(6\sigma)^2(2\pi)^3$	$(6\sigma)^2(2\pi)^2(7\sigma)^1$
$X^2\Pi$	$1^2\Sigma^-$	5.17	69	80	89	$(6\sigma)^2(2\pi)^3$	$(6\sigma)^2(2\pi)^2(7\sigma)^1$
$1^2\Sigma^+$	$^4\Pi$	4.31	65	19	64	$(6\sigma)^1(2\pi)^4$ $(6\sigma)^2(2\pi)^2(7\sigma)^1$	$(6\sigma)^1(2\pi)^3(7\sigma)^1$
$1^2\Sigma^+$	$1^2\Sigma^-$	3.60	7	6	25	$(6\sigma)^1(2\pi)^4$	$(6\sigma)^2(2\pi)^2(7\sigma)^1$
$1^2\Sigma^+$	$1^4\Sigma^-$	3.54	17	17	12	$(6\sigma)^1(2\pi)^4$	$(6\sigma)^2(2\pi)^2(7\sigma)^1$
$1^2\Delta$	$^4\Pi$	5.23	111	112	114	$(6\sigma)^2(2\pi)^2(7\sigma)^1$	$(6\sigma)^1(2\pi)^3(7\sigma)^1$

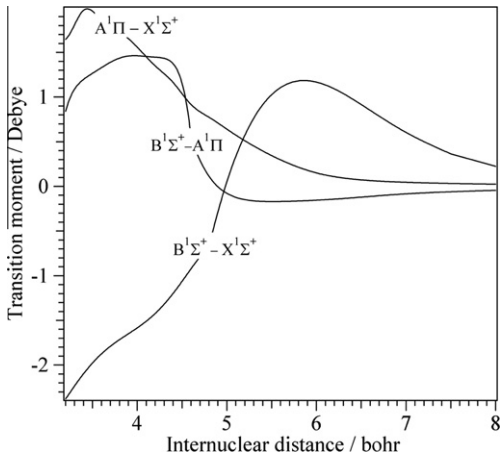

Fig. 7. Electronic transition moment functions between the $X^1\Sigma^+$, $A^1\Pi$ and $B^1\Sigma^+$states.

their corresponding lifetimes are reduced from the ns to the ps timescale because of spin-orbit predissociation.

4.2. Single photo-ionization spectrum of BeS

At both the (R)CCSD(T)/cc-pV5Z and CASSCF/MRCI/cc-pV5Z levels of theory, the ionization energy of BeS is computed to be 9.15 eV. It corresponds to the first peak in the spectrum of Fig. 8. This spectrum is deduced as follows: Our BeS ($X^1\Sigma^+$) PEC and those of the BeS^+ cation were incorporated into the LEVEL program to calculate the Franck–Condon factors for ionization transitions between BeS (v'' = 0, N'') populating the (v'^+, N'^+) ro-vibrational levels of BeS^+ in the $X^2\Pi$, $1^2\Sigma^+$, $1^2\Sigma^-$, $1^2\Delta$, $2^2\Sigma^+$, $2^2\Pi$ and $3^2\Pi$ states, whereas the quartet cationic states are not. Then, the transitions were fitted with a Gaussian function, with a full width at half maximum (FWHM) of 50 cm^{-1} (to simulate the resolution achieved by current available experiments) and a single photo-ionization spectrum has been simulated. We depict in Fig. 8 the corresponding spectrum. The abscissa is the energy relative to the BeS vibrational ground state. The "Q-Branch" approximation was adopted, i.e. only transitions with $\Delta N = 0$ were considered, and the line intensities were estimated by multiplying the calculated Franck Condon Factors by the relative population of each rotational level. With the adopted FWHM of 50 cm^{-1}, we fully resolve the vibrational structures for the transitions lying in the 9.15–15.4 eV.

The $X^2\Pi$ and $1^2\Sigma^+$ of BeS^+ are located in the middle of the Franck–Condon (FC) region (marked as a vertical solid line in Fig. 4), whereas the other electronic states present potential wells outside this region. The spectrum of Fig. 8 is dominated by the $BeS^+(1^2\Sigma^+, v'^+ = 0) + e^- \leftarrow BeS\ (X^1\Sigma^+, v'' = 0)$ transition because of favorable Franck–Condon overlap of the corresponding wavefunctions. Between 9.1 and 9.8 eV, we locate a long vibrational progression, which is associated with $BeS^+(X^2\Pi, v'^+) + e^- \leftarrow BeS(X^1\Sigma^+, v'' = 0)$. For energies greater than 11 eV, several vibrational bands involving higher lying excited states of BeS^+ may be observed. The spectrum is composed by well identified progressions in despite that the corresponding cationic states are closely lying in energy (Fig. 4). For the $BeS^+(2^2\Pi, v'^+) + e^- \leftarrow BeS\ (X^1\Sigma^+, v'' = 0)$ bands, we compute however weak transitions that will make hard their identifications in the experimental spectra whenever measured. More generally, the assignment of the experimental bands far from the ionization potential should be difficult because of congestion of the bands. This synthetic spectrum should be helpful to understand these experimental spectra.

Table 7
Variationally determined energies (in cm^{-1}) of the v' = 0 up to 33 vibrational levels of $BeS(A^1\Pi)$ and their lifetimes $\tau^{v'}$ including the radiative $\tau^{rad,v'}$ and the non-radiative $\tau^{non\text{-}rad,v'}$ ones. See text for more details. These lifetimes are in ns.

v'	E	$\tau^{rad,v'}$	$\tau^{non\text{-}rad,v'}$	$\tau^{v'}$
0	0.00	240.45		240.45
1	719.09	195.32		195.32
2	1423.56	171.44		171.44
3	2124.07	159.39		159.38
4	2823.97	152.12		152.12
5	3524.14	145.94		145.94
6	4224.55	139.74		139.74
7	4924.65	133.59		133.59
8	5624.01	127.55		127.55
9	6321.92	121.50		121.50
10	7016.85	115.85		115.85
11	7706.36	111.07		111.07
12	8387.39	107.25		107.25
13	9057.40	104.05		104.05
14	9715.31	101.10		101.10
15	10361.85	98.13		98.13
16	10999.10	95.06		95.06
17	11628.76	92.11		92.11
18	12251.21	89.39		89.39
19	12866.40	87.10		87.10
20	13473.77	85.12		85.12
21	14072.93	83.43		83.43
22	14663.92	82.28		82.28
23	15246.65	81.24		81.24
24	15821.23	80.10		80.10
25	16387.78	79.54		79.54
26	16946.23	79.56		79.56
27	17496.68	79.33		79.34
28	18039.11	78.63		78.64
29	18573.53	78.22		78.22
30	19099.95	78.70	188.75	55.54
31	19618.30	79.80	0.0662	0.066
32	20128.52	80.72	0.0006	0.0006
33	20630.39	80.97	0.0003	0.0003

5. Conclusions

Using *ab initio* methodology, we computed the BeS and BeS^+ potential energy curves of the low-lying electronic states and their

Table 8
Variationally calculated energies (in cm^{-1}) of the $v' = 0$ up to 19 vibrational levels of BeS ($B^1\Sigma^+$) and their lifetimes $\tau^{v'}$ including the radiative $\tau^{rad,v'}$ and the non-radiative $\tau^{non\text{-}rad,v'}$ ones. See text for more details. These lifetimes are in ns.

v'	E	$\tau^{rad,v'}_{B\to A}$	$\tau^{rad,v'}_{B\to X}$	$\tau^{rad,v'}$	$\tau^{non\text{-}rad,v'}$	$\tau^{v'}$
0	0.00	19.23	4.11	3.39		3.39
1	775.16	18.44	4.09	3.35		3.35
2	1581.05	16.84	4.2	3.36		3.36
3	2379.97	15.49	4.34	3.39		3.39
4	3163.46	14.5	2.45	2.09		2.09
5	3934.10	13.81	4.6	3.45		3.45
6	4695.33	13.32	2.6	2.17		2.17
7	5449.38	12.93	4.79	3.49		3.49
8	6198.01	12.60	4.87	3.51		3.51
9	6942.31	12.25	4.94	3.52	7.4	2.38
10	7683.46	11.86	2.74	2.22	0.02	0.02
11	8422.61	11.55	2.77	2.23	0.07	0.07
12	9160.64	11.61	2.81	2.26	0.04	0.04
13	9897.54	12.27	2.86	2.32	0.01	0.01
14	10631.34	13.64	2.91	2.40	0.06	0.06
15	11356.60	15.84	2.99	2.51	0.05	0.05
16	12062.36	18.66	3.13	2.68	0.05	0.05
17	12729.12	20.58	3.62	3.08	0.06	0.06
18	13329.91	22.48	4.31	3.62	0.07	0.07
19	13866.19	27.16	4.77	4.06	0.08	0.08

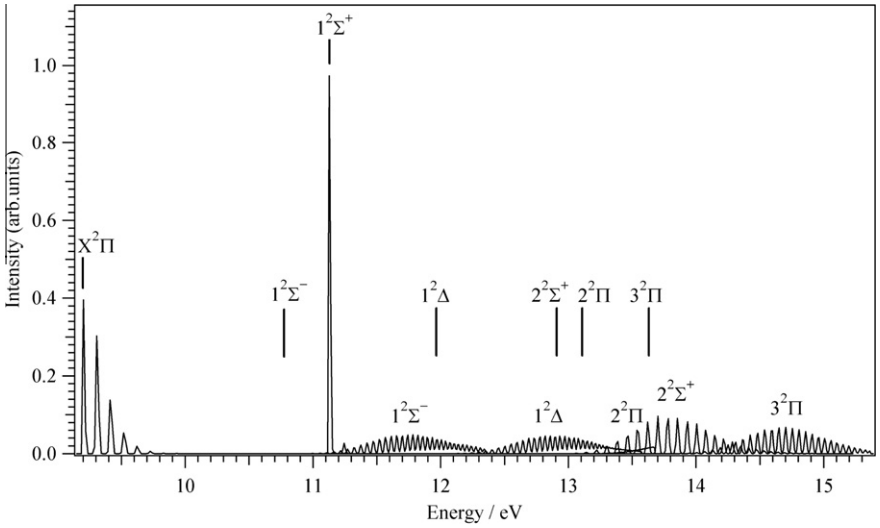

Fig. 8. Simulation of the ionization spectrum of the neutral BeS ($X^1\Sigma^+$). The vertical lines correspond to the band origins of the BeS^+ ($X^2\Pi$, $1^2\Sigma^-$, $1^2\Sigma^+$, $1^2\Delta$, $2^2\Sigma^+$, $2^2\Pi$ and $3^2\Pi$) states. We used a resolution of 50 cm^{-1}. See text for more details.

mutual transition moments and spin–orbit integrals. Then, accurate spectroscopic constants were deduced for the bound states of both species. For BeS, we found a good agreement with the available experimental data. The spin–orbit couplings and the allowed transition moments were used later, together with the PECs to calculate the radiative lifetimes of the vibrational levels of the $a^3\Pi$, $A^1\Pi$, $^3\Sigma^+$ and $B^1\Sigma^+$ states and to estimate the strength of the predissociation processes in the $X^1\Sigma^+$, $A^1\Pi$, and $B^1\Sigma^+$. These data should help to understand the eventual perturbations in the absorption spectra of BeS. For BeS^+, our results are predictive in nature and should be useful for identifying this cation in laboratory. Finally, the synthetic single ionization spectrum of BeS ($X^1\Sigma^+$) to populate the BeS^+ ($X^2\Pi$, $1^2\Sigma^-$, $1^2\Sigma^+$, $1^2\Delta$, $2^2\Sigma^+$, $2^2\Pi$ and $3^2\Pi$) states was evaluated.

Acknowledgements

Professor R.J. Le Roy is acknowledged for kindly providing us with the LEVEL and BCONT programs.

References

[1] N. Benosman, N. Amrane, S. Méçabih, H. Aourag, Phys. B 304 (2001) 214.
[2] D. Heciri, L. Beldi, S. Drablia, H. Meradji, N.E. Derradji, H. Belkhir, B. Bouhafs, Comput. Mater. Sci. 38 (2007) 609.
[3] D. Rached, M. Rabah, N. Benkhettou, R. Khenata, B. Soudini, Y. Al-Douri, H. Baltache, Comput. Mater. Sci. 37 (2006) 292.
[4] C. Jing, C. Xiang-Rong, Z. Wei, Z. Jun, Chin. Phys. B 17 (2008) 1377.
[5] W.J.M. Gissane, R.F. Barrow, Proc. Phys. Soc. 82 (1963) 1065.
[6] C.J. Cheetham, W.J.M. Gissane, R.F. Barrow, Trans. Frad. Soc. 61 (1965) 1308.
[7] G. Verhaegen, W.G. Richards, Proc. Phys. Soc. 90 (1967) 579.
[8] B. Pouilly, J.M. Robbe, J. Schamps, R.W. Field, L. Young, J. Mol. Spectrosc. 96 (1988) 1.
[9] J. Noga, T. Pluta, Chem. Phys. Lett. 264 (1997) 101.
[10] H. Ghalila, S. Lahmar, Z. Ben lakhdar, M. Hochlaf, J. Phys. B: At. Mol. Opt. Phys. 41 (2008) 205101.
[11] R.J. Buenker, H.-P. Liebermann, L. Pichel, M. Tachikawa, M. Kimura, J. Chem. Phys. 126 (2007) 104305.
[12] MOLPRO is a package of *ab initio* programs written by H.-J. Werner and P.J. Knowles; further details at <http://www.molpro.net>.
[13] T.H. Dunning Jr., J. Chem. Phys. 90 (1989) 1007.
[14] D.E. Woon, T.H. Dunning Jr., J. Chem. Phys. 98 (1993) 1358.
[15] P.J. Knowles, H.-J. Werner, Chem. Phys. Lett. 115 (1985) 259.
[16] H.-J. Werner, P.J. Knowles, J. Chem. Phys. 82 (1985) 5053.

[17] H.-J. Werner, P.J. Knowles, J. Chem. Phys. 89 (1988) 5803.
[18] P.J. Knowles, H.-J. Werner, Chem. Phys. Lett. 145 (1988) 514.
[19] S.R. Langhoff, E.R. Davidson, Int. J. Quantum Chem. 8 (1983) 61.
[20] The code NUMEROV used in the present application was written by J. Senekovitsch et al., Johan Wolfgang Goethe Universität, Frankfurt, Germany.
[21] J.W. Cooley, Math. Comput. 15 (1961) 363.
[22] R.J. Le Roy, LEVEL 7.2, University of Waterloo, Chemical Physics Research Report CP-642, 2002.
[23] R.J. LeRoy, BCONT, University of Waterloo, Chemical Physics Research Report CP-329R3, 1993.
[24] H. Lefebvre-Brion, R.W. Field, The Spectra and Dynamics of Diatomic Molecules, Elsevier, 2004.
[25] V. Brites, D. Hammoutène, M. Hochlaf, J. Phys. B 41 (2008) 045101.
[26] http://webbook.nist.gov/chemistry/.